Concept Design of a Multi-Band Shared Aperture Reflectarray/Reflector Antenna

Thomas Spence, Michael Cooley, Peter Stenger, Richard Park
Northrop Grumman Mission Systems (NGMS)
Baltimore, MD USA
thomas.spence@ngc.com

Lihua Li, Paul Racette, Gerald Heymsfield, Matthew Mclinden
NASA Goddard Space Flight Center (GSFC)
Greenbelt, MD, USA

***Abstract*— A scalable dual-band (Ka/W) shared-aperture antenna system design has been developed as a proposed solution to meet the needs of the planned NASA Earth Science Aerosol, Clouds, and Ecosystem (ACE) mission. The design is comprised of a compact Cassegrain reflector/reflectarray with a fixed pointing W-band feed and a cross track scanned Ka-band Active Electronically Scanned Array (AESA). Critical Sub-scale prototype testing and flight tests have validated some of the key aspects of this innovative antenna design, including the low loss reflector/reflectarray surface.**

More recently the science community has expressed interest in a mission that offers the ability to measure precipitation in addition to clouds and aerosols. In this paper we present summaries of multiple designs that explore options for realizing a tri-frequency (Ku/Ka/W), shared-aperture antenna system to meet these science objectives. Design considerations include meeting performance requirements while emphasizing payload size, weight, prime power, and cost. The extensive trades and lessons learned from our previous dual-band ACE system development were utilized as the foundation for this work.

Keywords*— *Reflectarrays, Reflectors, Phased Arrays, Millimeter Wave, NASA Earth Science

I. Background

A high efficiency, dual-band (Ka/W), shared-aperture antenna system design has been developed for NASA's planned Aerosol, Climate, and Ecosystem (ACE) mission [1-4]. The architecture provides a fixed nadir beam at W-band and a cross-track scanning beam at Ka-band using the same primary parabolic cylinder reflector. The enabler for this design is the low loss reflectarray surface on the primary reflector. For Ka-band operations the antenna is fed by an Active Electronically Scanned Array (AESA) line feed at the virtual focal line of the primary reflector (Cassegrain optics). The line feed provides polarimetric information via dual-linear polarized receive beams. For W-band operations a dual-pol beam waveguide system is located at the virtual focal point of the reflector. The reflectarray surface focuses the W-band energy in azimuth and elevation to/from the main reflector. It also enables the two bands to have co-aligned beams with separate feeds and sub-reflectors. This is discussed in greater detail in [1-3]. A model of the 7 square meter shared-aperture design is shown in Fig. 1. The feed and reflector designs are modular and scalable and can be adapted to meet evolving sensor/mission requirements and/or orbit altitudes. We have specifically addressed aperture sizes ranging from 7-17 square meters in our analyses and design trades to date, but emphasized the smaller aperture to minimize cost and SWaP (size, weight, & power). This range was primarily selected based on the requirements and goals of system sensitivity, horizontal resolution and doppler accuracy at Ka- and W-band, as well as the spacecraft size constraint.

A sub-scale antenna was fabricated, tested, and flown on the NASA ER-2 aircraft to demonstrate the viability of the ACE mission antenna system. The sub-scale antenna, shown in Fig. 2, is an offset-fed parabolic cylinder with an aperture size of 61 cm x 61 cm and the same f/D as the full scale ACE design (Fig. 1). At Ka-band it is fed by a fixed beam line array of dual-pol patch antennas at the focal line of the reflector. AESA-based beam steering was replicated and validated by swapping among a set of scanned, fixed beam line feeds during range testing. For W-band operations a dual-pol horn is located at the virtual focal point of the reflector and a reflectarray surface focuses its energy in azimuth and elevation.

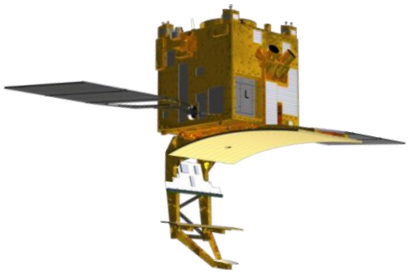

Fig.1. Model of the dual-band, shared-aperture antenna architecture for the ACE mission.

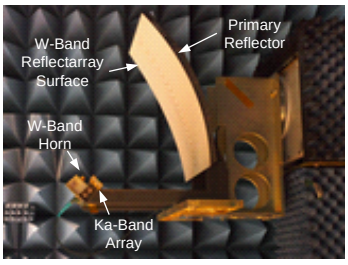

Fig. 2. The sub-scale antenna installed on a support pedestal in a compact antenna range.

This work was funded through the Instrument Incubator Program (IIP) through NASA's Earth Science and Technology Office (ESTO).

The performance of the sub-scale antenna was successfully measured in a compact antenna range at NASA GSFC in Greenbelt, MD. Measured to modeled agreement was very good. Gain contour plots in vicinity of the main beam for the antenna at Ka-band are shown in Fig. 3. In this particular configuration the patch line feed is phased to direct the beam ten degrees off nadir in the cross-track direction (i.e., along its length). As expected, at Ka-band the reflector/reflectarray surface serves as a reflector since the reflectarray surface is essentially RF transparent at this frequency. The tapered amplitude distribution of the line feed provides low side lobes in the cross-track direction. The parabolic cylinder reflector focuses the line feed pattern in the along-track direction and the associated amplitude taper lowers the along-track side lobes and increases the antenna gain.

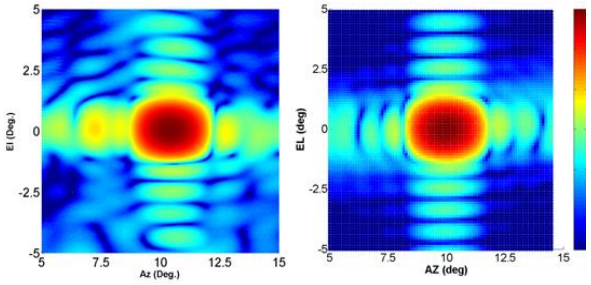

Fig. 3. Measured (left)and predicted (right) normalized gain contour plots (35.55 GHz) near the main beam of the subscale antenna with its beam directed to ten degrees off boresight.

Measured and predicted gain contour plots in the vicinity of the main beam at 94.05 GHz are shown in Fig. 4. Very good agreement is observed. The reflectarray surface on the parabolic cylinder collimates the incident energy of the W-band waveguide feed horn and aligns the main beam with that of the Ka-band nadir beam.

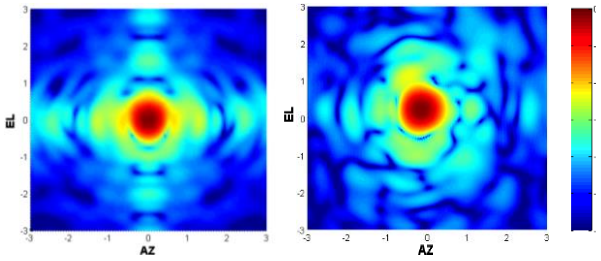

Fig. 4. (Left) Measured and (right) predicted normalized gain contour plots (94.05 GHz) near the main beam of the subscale antenna.

During the NASA Integrated Precipitation and Hydrology EXperiment (IPHEX, 2014) and the NASA Olympic Mountains Experiment (OLYMPEX, 2015)/Radar Definition Experiment (RADEX) field missions, the sub-scale antenna was installed on the NASA ER-2 aircraft (Fig. 5) and used for high altitude, sub-orbital radar measurements at W-band [5]. It was paired with NASA GSFC's 94 GHz Cloud Radar System (CRS) for high resolution Doppler measurements. Concurrent, co-located data collection was also performed at additional frequencies (X, Ku, & Ka) using other NASA GSFC radar systems on the same aircraft.

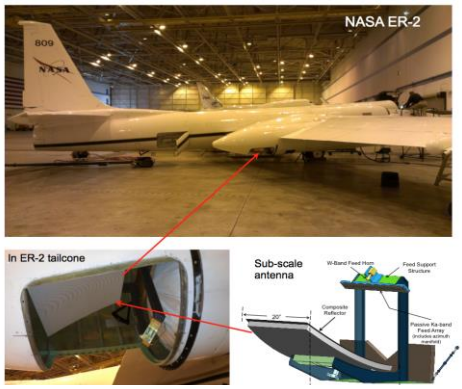

Fig. 5. Radar reflectivity and Doppler velocity data were collected on the NASA ER-2 aircraft. The sub-scale antenna was used for the W-band data collection during the NASA IPHEX and OLYMPEX/RADEX missions.

II. Driving Requirements

The antenna architectures presented in this paper are supporting a NASA tri-band imaging radar concept called the Cloud and Precipitation Process Mission (CaPPM) [6]. They leverage the ACE dual-band architecture, technologies, and analysis tools developed and the successful sub-scale proof of concept demonstrator that were described in Section I. The tri-band radar is aimed at measuring reflectivity, Doppler, and polarimetric data of clouds and precipitation from the earth's atmosphere. Retrieval products include data such as particle size, rain rate, and weather system dynamics. The shared-aperture tri-frequency antenna system provides wide swath imaging at Ka-band (120 km) and Ku-band (250 km), and can provide either fixed beam (via use of a reflectarray on the main reflector) or cross-track scanning (via use of an AESA line feed) at W-band.

The primary performance metric for the radar system is sensitivity. From an antenna design standpoint the principal parameters impacting radar performance are radiated power, gain, beamwidth, and the two-way side lobe level. Striking a balance between size, weight, prime power, cost, complexity, and technology readiness level are also factored into the overall system design.

From a capability standpoint the architectures considered can be grouped into two main categories: Category 1 includes those providing Ku/Ka-band scanning and a W-band fixed nadir beam, and Category 2 includes those providing tri-frequency scanning capability. An additional subgroup is comprised of architectures providing dual-band scanning at Ka- and W-band.

System budgets were developed for a number of CaPPM radar concepts to explore the design trade space. Included in the trade space were parameters such as capability (i.e., architecture categories 1 & 2), antenna aperture size, swath scanning flexibility (e.g., scanning vs. nadir dwelling), and RF/prime power. A case study of a CaPPM radar concept

system budget is shown in Table 1. In this example the budget is based on a 7 m^2 antenna aperture from Category 1. Detailed losses through the full RF chain were included.

TABLE 1. CaPPM key radar system parameters with a 7 m^2 antenna aperture.

Parameters	CaPPM		
Frequency (GHz)	13.48	35.56	94.05
Orbit Altitude (km)	395-420		
Transmitter	SSPA	SSPA	EIK
Tx Peak Power (W)	2000	2200	1800
Antenna Size (m)	3.0x2.3	3.0x2.3	3.0x2.3
PRF (Hz)	4700	4700	4700
Vertical Res. (m)	250	250	250
Horizontal Res. (km)	5.0x4.0	2.0x1.5	0.75x1.0
Cross Track Swath (km)	250	120	0.75
Nadir MDZ (dBZ)	1.0	-13.2	-33.6
Swath MDZ (dBZ)	4.0	-10.2	N/A
Doppler Vel. Accuracy (m/s)	1.0	0.5	0.2
Polarization Option	Yes	Yes	Yes

III. Antenna System Design

As shown in Table 2, numerous antenna architectures were identified and explored to establish leading candidate architectures within Categories 1 and 2. Primary emphasis was placed on the overall aperture design (type of optics, f/D, feed design & placement, etc.) as well as the AESA transmit/receive (T/R) modules (device technology, power requirements, packaging, etc.).

X/Ku band AESA T/R module technologies have very high TRLs based on significant production heritage for various radar applications and platforms. Ka-band AESA T/R module technologies are also relatively mature with a variety of systems in various stages of development and deployment. W-band AESA T/R module technologies are just now beginning to emerge. Architecture trades for spaceflight programs such as CaPPM need to include careful assessments of TRLs, development timelines and associated expected performance (e.g. high power amplifier (HPA) RF output power and DC-to-RF conversion efficiency are especially important).

TABLE 2. High level overview of the antenna architecture trade space addressed.

Sub Category	Category1 Ku/Ka Scanning & W Fixed Beam	Category 2 Ku/Ka/W Scanning
A	Ku/Ka Sub-Reflector (Parabolic Cylinder) W Sub-Reflector (Doubly Curved) *Ku-Band*: De-Focused line feed. *Ka-Band*: Line feed on focal line of sub. *W-Band*: RA surface on primary reflector provides point focusing. BWG system folds optics behind reflector.	Single Sub-Reflector (Parabolic Cylinder) *Ku-Band*: De-Focused line feed. *Ka-Band*: De-focused line feed. *W-Band*: Line feed on focal line of sub.
B	Ku/Ka Sub-Reflector (Parabolic Cylinder) W Sub-Reflector (Doubly Curved) *Ku-Band*: Line feed on focal line of sub. *Ka-Band*: De-Focused line feed. Beam squint/aberration corrected via RA on sub. *W-Band*: RA surface on primary reflector provides point focusing. BWG system folds optics behind reflector.	Single Sub-Reflector (Parabolic Cylinder) *Ku-Band*: De-Focused line feed. *Ka-Band*: Line feed on focal line of sub. *W-Band*: De-Focused line feed. Beam squint/aberration corrected via RA on sub.
C	N/A	Single Sub-Reflector (Parabolic Cylinder) *Ku-Band*: Line feed on focal line of sub. *Ka-Band*: De-Focused line feed. De-Focused line feed. Beam squint/aberration corrected via dual-band RA on sub. *W-Band*: De-Focused line feed. Beam squint/aberration corrected via dual-band RA on sub.
D	N/A	Single Sub-Reflector (Parabolic Cylinder) *Ku-Band*: Line feed on focal line of sub. *Ka-Band*: Line feed on focal line of sub. Interleaved Ku & Ka line feed array elements; separate T/R modules. *W-Band*: De-focused line feed. Beam squint/aberration corrected via RA on sub.
E	N/A	Single Sub-Reflector (Parabolic Cylinder) *Ku-Band*: Line feed on focal line of sub. *Ka-Band*: Line feed on focal line of sub. Dual-band Ku & Ka feed array and T/R modules. *W-Band*: De-focused line feed. Beam squint/aberration corrected via RA on sub.
F	N/A	Two Sub-Reflectors (Parabolic Cylinders) *Ku-Band*: Line feed on focal line of sub 1. *Ka-Band*: Line feed on focal line of sub 2. *W-Band*: De-focused line feed. Beam squint/aberration corrected via RA on sub 2.
RA – Reflectarray BWG – Beam Waveguide		

A. *Antenna Aperture Design*

The ACE antenna architecture [1-4] was the starting point when considering options for adding Ku- and/or W- band AESA scanning capability. Determining how to best incorporate these AESAs into a shared-aperture design was one of the primary objectives. The design trade space included a number of options such as using single- or dual-band AESA line feeds, feed placement possibilities, and utilizing shared sub-reflectors.

In nearly every tri-band architecture identified, one or more AESA line feeds must be displaced from the focal line of the parabolic cylindrical reflector; the aberrations caused by the displacement result in a gain reduction, sidelobe degradation, and band-to-band beam misalignment. The low loss reflectarray surface and synthesis tools developed for the ACE antenna design [1–3] were the foundation for correcting for these aberrations and in opening the design space for feed placement options. This technology enables two or more

AESA line feeds to share the same reflector and subreflector with high efficiency, no pattern distortion, and co-aligned beams. Attaining co-aligned beams is attractive for the tri-band radar because it allows for simultaneous collection of retrieval products at all three bands in the same concentric atmospheric volume.

Antenna aperture size is one of the key trade space parameters for any large aperture antenna design. Primary focus was placed on apertures between 7 m^2 to 17 m^2. At the low end of this range the gain of the antenna ranged from approximately 50 dBi at Ku-band to 67 dBi at W-band. These values take into account all pertinent front-end antenna losses. The beamwidth in the along-track (AT) and cross-track (CT) directions are also tied to the antenna aperture size. These beamwidths directly drive the spatial resolution of the system and the number of integrated pulses within a scan swath.

Within Category 1 there are various architecture trades for achieving Ku/Ka-band scanning and a W-band nadir beam. Trades include design details such accepting degraded performance of a feed displaced from the focal line versus correcting for this via a reflectarray/reflector surface on a subreflector. Separate AESA line feeds targeting individual operating bands versus dual-band AESA line feeds were also considered; performance, complexity, flexibility, and prime power are some of the important factors to consider. Ultimately two primary candidates were selected within Category 1. An example model of one of the candidates is shown in Fig. 6.

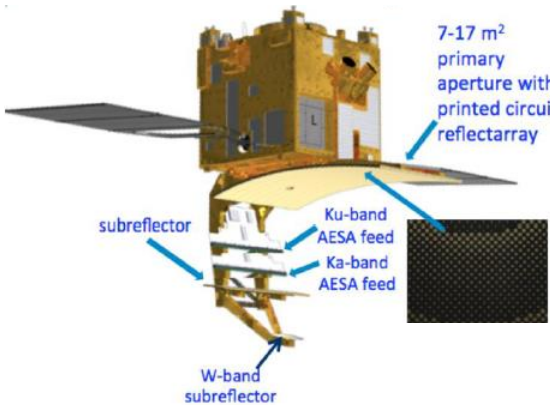

Fig. 6. Model of a tri-band, shared-aperture antenna concept for CaPPM.

The RF model of one of the down selected Category 1 candidates is shown in Fig. 7. This configuration closely mimics the ACE dual-band (Ka/W) design discussed in Section I. Here, an additional Ku-band line feed AESA is added next to the Ka-band feed, which resides on the focal line of the subreflector. Aberrations due to the defocused Ku-band feed result in a two-way loss of approximately 0.4 dB. In addition, the beam squints in the along-track direction and is not coincident with the Ka and W beams. Employing a Ku feed on the focal line and a displaced Ka feed (swapping the Fig. 7 Ku and Ka feed locations) with a Ka reflectarray surface on the subreflector to correct for beam squint would provide coincident beams at all three bands. Representative cuts of the two-way pattern of the (7 m^2) antenna when the Ku-band feed is on the focal line are shown in Fig. 8.

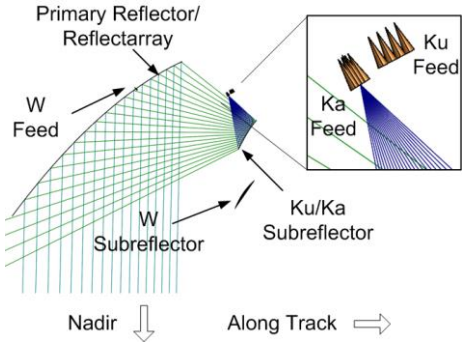

Fig.7. View of an RF model used on the assessment of one of the primary candidates of Category 1.

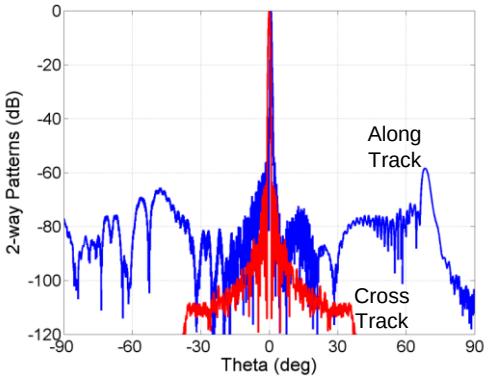

Fig. 8. Modeled 2-way side lobe patterns in the cross- and along-track direction for the 7 m^2 aperture at Ku-band (13.6 GHz).

Within Category 2 a number of candidate architectures were identified and assessed to provide a shared-aperture, tri-band scanning antenna. For Category 2 the W-band beam waveguide and its associated subreflector are replaced by an AESA line feed. The packaging and mechanical design complexity is mitigated by sharing the same parabolic subreflector among the three AESA feeds. Many of trades within this category are similar to those of Category 1. Complexity, cost, prime power, and technology maturity are especially important considerations for this category.

A notional illustration of one of the down selected Category 2 candidates is shown in Fig. 9. Three individual AESA line feeds share the same subreflector and primary reflector. The Ka-band feed is placed on the focal line of the subreflector. The W-band feed is placed next to the Ka-band feed and its defocusing is corrected via a W-band reflectarray surface on the subreflector. The Ku-band feed resides on the opposite side of the Ka-band feed. The W-band reflectarray surface is virtually RF transparent at Ku- and Ka-bands and at these frequencies the subreflector behaves like a conventional reflector surface. Representative cuts of the two-way pattern of the (7 m^2) antenna at W-band are shown in Fig. 10.

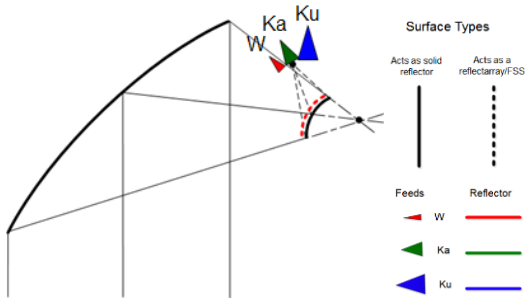

Fig.9. View of an RF model used on the assessment of one of the primary candidates of Category 2.

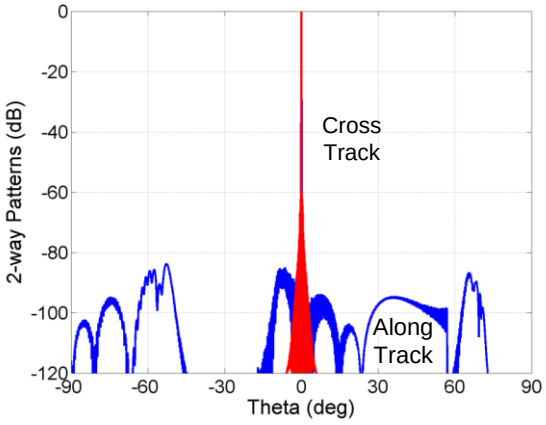

Fig. 10. Predicted 2-way side lobe patterns in the cross- and along-track direction for the 7 m^2 aperture at W-band (94.0 GHz).

B. AESA T/R Module Design

The AESA T/R modules are a critical component of the tri-band radar system. NGMS and GSFC are currently developing a Ka-band T/R module that addresses the design requirements of the ACE mission; this work is funded by NASA's Earth Science and Technology Office (ESTO) through the Instrument Incubator Program (IIP). The scope of this T/R module development work includes T/R module RF and mechanical design as well fabrication and test of key devices such as the GaN HPA MMIC, the LNA/switch MMIC, the multi-function control and T/R MMICs, an integrated circulator and a gate/power control ASIC. This tailored module design was optimized to yield high radar sensitivity and very low DC power consumption in a compact package. The architecture trades and design details associated with this module, as well as the extensive experience of NGMS in the area of production AESAs, were leveraged to develop concepts and identify design trades for Ku and W-band modules.

Primary trades for the T/R modules included the device technology, RF front-end architecture, layout, and packaging. Conceptual layouts were created for the Ku- and W-band modules. These were used to explore the form, fit, and function of key components (such as high power amplifiers and low noise amplifiers) and to examine the space required for adjacent line feeds. A mechanical model of adjacent AESA line feeds that are associated with Category 1 and 2 trades is shown in Fig. 11. A detailed mechanical layout of the Ka-band T/R module and a front end RF block diagram are also shown.

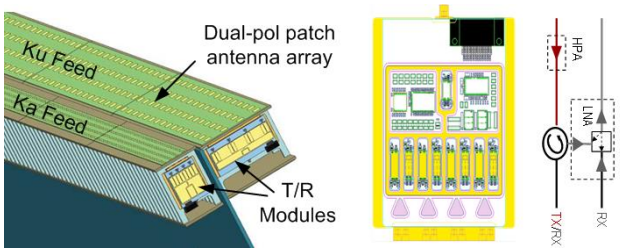

Fig.11. (Left) Modeled view of adjacent Ka and Ku AESA line feeds and (right) detailed layout of the Ka module and its block diagram.

Management of tolerances and errors is a critical for AESA designs and is especially important for the CaPPM radar wherein a very low two-way side lobe level is required to minimize the effects of an earth ground return. CaPPM requires a maximum two-way side lobe level of -76 dB in order to minimize the earth return clutter within a desired range gate.

Component variability and device resolution (amplitude and phase quantization) tend to be the dominant AESA error sources that impact side lobe level. Array element failures are also an important design consideration throughout the system lifecycle. Failed individual elements or T/R modules perturb the nominal AESA amplitude and phase distributions and degrade the antenna pattern. NGMS is leveraging extensive experience in AESA tuning and failure mitigation in the architecting of the tri-band antenna system. This includes techniques employed during initial integration and test as well as "in the field" techniques that have been proven on multiple production AESA-based radar systems.

Detailed analyses were performed to understand the role of errors in the various architecture categories under consideration for the tri-band system. An example of the outputs of a case study for the Ka-band AESA line feed of a 7 m^2 aperture antenna is shown in Fig. 12 and 13. Expected component tolerances and device quantization were included in the analysis. Tuned transmit and receive patterns were calculated through a Monte Carlo simulation and results and statistics were analyzed. The cumulative distribution of the analysis indicates the design meets the targeted -76 dB two-way side lobe level.

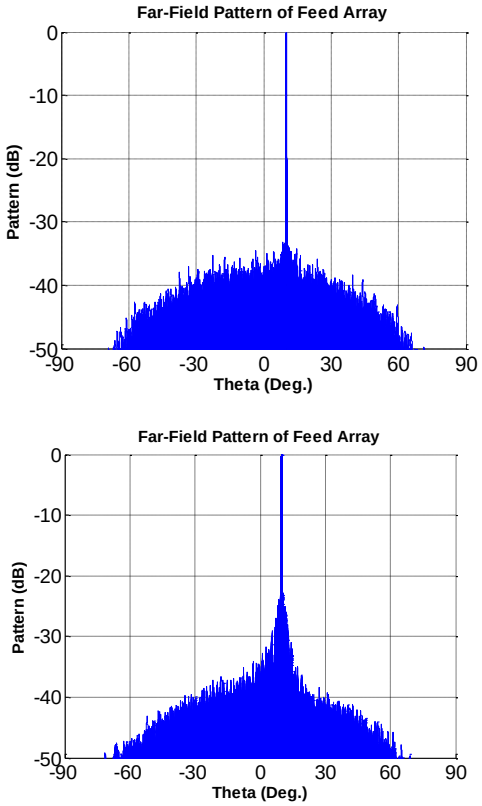

Fig. 12. Overlay of normalized cross-track pattern cuts from a Monte Carlo analysis of a 7 m^2 antenna with a Ka-band AESA line feed. (Upper) Receive pattern and (Lower) transmit patterns are shown.

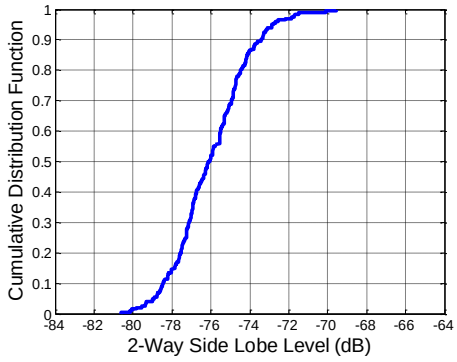

Fig. 13. Cumulative distribution function of the two-way side lobe level from a Monte Carlo analysis of a 7 m^2 antenna with a Ka-band AESA line feed.

IV. Summary

This paper describes antenna system architecture concepts developed in support of a NASA tri-band cloud /precipitation imaging radar concept called the Cloud and Precipitation Process Mission. This development leverages the dual-band (Ka/W) shared-aperture antenna system concept, technologies, and analysis tools previously developed for the NASA ACE mission, including the sub-scale antenna flown on the NASA ER-2 aircraft along with the NASA GSFC 94 GHz Cloud Radar System for 30 science flights.

From a capability standpoint the architectures considered can be grouped into two main categories: Category 1 includes those providing Ku/Ka-band scanning and a W-band fixed nadir beam, and Category 2 includes those providing tri-band scanning capability. Striking a balance between performance, size, weight, prime power, cost, complexity, and technology readiness level were factored into the overall system designs.

Antenna system architecture trades placed primary focus on the reflector and AESA line feed technology. The design space includes a number of options such as using single- or dual-band AESA line feeds, feed placement possibilities, and utilizing shared sub-reflectors. Additionally, trades explored for the AESA T/R modules include the device technology, RF front-end architecture, layout, and packaging.

Acknowledgements

The authors would like to thank NASA's Earth Science and Technology Office for their funding which has enabled the development of these antenna designs and supporting technologies.

References

[1] M. Cooley, et al., "Dual-Band Reflector/Reflectarray: A Novel Antenna Architecture for the NASA ACE Radar," AIAA Space Symposium, Long Beach, CA, Sept. 2011.

[2] T. Hand, et al., "Dual-band shared aperture reflector/reflectarray antenna: Designs, technologies and demonstrations for nasa's ACE radar," *IEEE Phased Array Symp. & Tech.*, Boston, MA, Oct.2013.

[3] P. Racette, et al., "Antenna Technologies Enable Wide-swath Imaging with the ACE Radar," *NASA 2014 Earth Science Technology Forum*, Leesburg, VA, Oct. 2014.

[4] L. Li, et al., "Wide-swath Shared-aperture Cloud Radar (WiSCR) ," *NASA 2015 Earth Science Technology Forum*, Pasadena, CA, June 2015.

[5] M. McLinden, et al.,"The Development and Performance of the NASA/GSFC W-band (94 GHz) Solid-State Cloud Radar System" *37th Conference on Radar Meteorology*, Norman, OK, Sept. 2015.

[6] L. Li, et al., "A Multi-frequency Wide-Swath Spaceborne Cloud and Precipitation Imaging Radar," *96th American Meterological Society Annual Meeting*, New Orleans, LA, Jan. 2016.